Rare Metal Materials and Engineering
Volume 47, Issue 6, June 2018
Online English edition of the Chinese language journal

Available online at www.sciencedirect.com

Cite this article as: Rare Metal Materials and Engineering, 2018, 47(6): 1682-1688.

ARTICLE

Acetone Gas Sensing Properties of Au-activated Ni-doped ZnO Nanoparticles Prepared by Coprecipitation Method

Wang Jinxiao[1,2], **Yang Jun**[1], **Han Ning**[2,3], **Yang Jianfeng**[4]

[1] Xi'an University of Architecture and Technology, Xi'an 710055, China; [2] State Key Laboratory of Multiphase Complex Systems, Institute of Process Engineering, Chinese Academy of Sciences, Beijing 100190, China; [3] Center for Excellence in Regional Atmospheric Environment, Institute of Urban Environment, Chinese Academy of Sciences, Xiamen 361021, China; [4] State Key Laboratory for Mechanical Behavior of Materials, Xi'an Jiaotong University, Xi'an 710049, China

Abstract: Pure and Ni-doped ZnO were prepared by a coprecipitation method, and the gas sensing properties were compared using 20 μg/g acetone. The results show that the optimal Ni doping concentration is 1 mol% with the highest response of 12 μg/g to 20 μg/g acetone. On this basis, Au was decorated onto Ni-doped ZnO to further improve the gas response. The results show that 0.03 mol% Au activated 1 mol% Ni-doped ZnO has the highest acetone gas response (about 17 μg/g to 20 μg/g) in all sensors, and it also maintains high selectivity over ethanol, formaldehyde and benzene, and rapid response-recovery time of <10 s.

Key words: acetone gas sensor; Ni doped ZnO; Au-activation; response-recovery time

Due to the advantages of high sensitivity and low cost, metal oxide (MOX) semiconductor gas sensors have become one of the research focuses with applications in inflammable gases alarming, environmental pollutants detection as well as in breath analysis for diseases. For example, acetone is believed to be one typical breath gas of the diabetes with higher concentrations in ppm level than normal ones in ppb level. Therefore, it is highly desired to develop highly sensitive materials for detection of low concentration gases.

The researches on gas sensors are mainly focused on the tailoring of crystallite, structure, morphology control, doping etc. of metal oxide semiconductor materials in the past few years [1-8]. Among the metal oxides, ZnO is extensively investigated for all kinds of gas-sensing application owing to its low cost and simple preparation[9-13]. It is found that the gas sensing property of ZnO is related to their chemical composition, morphologies and microstructures. Till now, ZnO nanowires[14], nanorods[15], nanobelts[16], nanotubes[17], and nanosheets[18] are all synthesized for gas sensors.

It is generally known that the gas sensing performance of samples is relevant to adsorption and desorption of oxygen ions, which is dependent on the adjustment and optimization of microstructure and morphology. But the technique of morphology and microstructure control is sophisticated and expensive. Other studies have been focused on the use of transition elements doping like Fe[19], Mn[20], Co[21]. Doping leads to more defects in the crystal, and there may be special reaction mechanisms between different doping elements and oxygen ions. In addition, noble metals[18,22] are usually used to activate MOX sensors as the second phase forming heterojunction, such that noble metals tend to promote oxygen adsorption. One of those is Au[23] which is used to activate ZnO to enhance the gas sensing property.

Nickel (3+) has similar ionic radius (~0.056 nm) to Zn^{2+} (0.06 nm) and thus can be easily doped into ZnO lattice forming a donor contributing electrons and favoring gas sensing performance. In this study, Ni-doped ZnO nanoparticles were prepared by a precipitation method and the structure, morphology, crystalline quality were investigated by

---

Received date: June 14, 2017
Foundation item: National Key Basic Research and Development Program of China ("973"Program) (2016YFC0207101); National Natural Science Foundation of China (11575228); State Key Laboratory of Multiphase Complex Systems (MPCS-2014-C-01)
Corresponding author: Yang Jun, Ph. D., Professor, School of Metallurgical Engineering, Xi'an University of Architecture and Technology, Xi'an 710055, P. R. China, E-mail: yj-yangjun@xauat.edu.cn

a series of characterizations. Then the acetone gas sensing properties of pure and Ni-doped ZnO sensors were compared, and an optimized Ni doping concentration of 1 mol% was obtained. Finally, Au was added into Ni-doped ZnO to further activate the materials and enhance the acetone sensing performance, including improved response and selectivity over ethanol, formaldehyde and benzene.

1 Experiment

1.1 Preparation of pure ZnO and Ni-doped ZnO

The 50 mL zinc sulfate heptahydrate (43.05 g) solution (with or without nickel nitrate) was added dropwise into 100 mL ammonium acid carbonate (9.984 g) solution. This process was carried out under the condition of water bath at 40 °C. The obtained precipitate was aged for 1 h, and was washed with water and ethanol several times and then was dried in an oven at 80 °C. The obtained precursor was calcined at 500 °C for 2 h in a tube furnace under air atmosphere to get the product.

In Au activation, Ni-doped ZnO was added into 0.4 mmol/L $HAuCl_4$ solution, with the molar ratio (Au/Zn) of 0.003%, 0.015%, 0.03% and 0.06%. The mixture was then ultrasonically dispersed, and dried in the oven at 100 °C. The mixture was calcined at 500 °C for 2 h in a tube furnace under air atmosphere to get the product.

1.2 Characterization

The morphologies of all the samples were observed by a SEM (scanning electron microscopy, JSM-7001F, Japan, 30 kV, 10 μA). The structure type and crystalline phases were identified using XRD (X-ray diffraction, Panalytical X'pert Pro, The Netherlands, Cu Kα radiation of λ=0.154 06 nm, 40 kV, 40 mA). The Raman spectra were measured on micro confocal Raman spectroscopy at room temperature (532 nm argon laser, Invia-Reflex 20 mW, Britain). The surface elements were measured on an X-ray photoelectron spectroscopy (XPS, ESCALab220i-XL) and Fourier transform infrared spectroscopy (FTIR, Excalibur 3100, America, between 4000 and 400 cm^{-1}).

1.3 Fabrication of sensors

The instrument for gas sensitivity test is WS-30A Gas sensor test system (Winsen Electronics Co. Ltd., China) as shown in Fig.1. The ZnO sample was ultrasonically dispersed in ethanol and was extracted with a micro-syringe to dribble onto the surface of a ceramic tube. A pair of Au electrodes had been installed at each end of the tube, and a Ni-Cr heating wire went through the tube to serve as a heating filament to control the operating temperature by tuning the heating voltage.

The gas response was defined as the ratio of the R_a/R_g[24], where R_a and R_g are the resistances of the sensor in air and tested gas, respectively. The response and recovery time were defined as the time taken by the sensor to achieve 90% of the total resistance change in the case of adsorption and desorption, respectively.

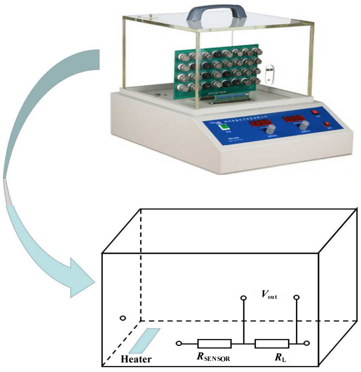

Fig.1 Diagram of WS-30A gas sensor test system set up

2 Results and Discussion

2.1 Structural and morphological characterization of pure and Ni-doped ZnO

Fig.2a shows the XRD patterns of the pure ZnO and 0.2 mol%, 0.5 mol%, 1 mol%, 2.2 mol% and 5 mol% Ni-doped ZnO. All the samples exhibit a hexagonal wurtzite structure and there are no other peaks appearing in these patterns. It suggests that the Ni element may be doped into ZnO lattice[25], as Ni^{2+} (0.49 nm) or Ni^{3+} (0.56 nm) has smaller ionic radius than Zn^{2+} (0.6 nm). However, when Ni doping level is as high as 5 mol%, the lattice will be distorted as illustrated by the wider and weaker XRD peaks[26]. FTIR spectra of samples are shown in Fig.2b. The stretching mode of Zn-O is observed at around 445 cm^{-1}. The vibration mode at 1128 cm^{-1} is relevant to Ni^{2+} replacing Zn^{2+}, because the difference between Ni and Zn radius leads to lattice distortion[26]. The FTIR results are in good agreement with the ones by XRD.

The Raman spectra of samples are shown in Fig.2c. It is clear that there are no impurity peaks emerging in these spectra in good agreement with XRD results. The E_{2H} of Ni-doped ZnO is slightly shifted compared with that of pure ZnO, which shows the vibration frequency change by the Ni^{2+} dopants in the ZnO lattice[27].

Fig.3 shows the SEM images of pure and Ni-doped ZnO, which have similar particulate morphology of about 50 nm. To further study the chemical composition and bonding state of Ni-doped ZnO, XPS analysis was conducted to give more direct evidence of the substitutional effects of Ni. The results are shown in Fig.4. All data are corrected with respect to the standard peak of C1s at 284.6 eV. It is clear that no extra peaks corresponding to any other impurity atoms are detected.

Fig.4a is the spectra of O 1s. According to previous reports, the asymmetric nature of peaks could be the presence of various bonding states of oxygen. The peak at 530.4 eV is attributed to O^{2-} in wurtzite structure. The peak at 532.4 eV is due to presence of hydroxyl groups on the surface[28]. The binding energy positions of Zn $2p_{3/2}$ and Zn $2p_{1/2}$ are 1021.27

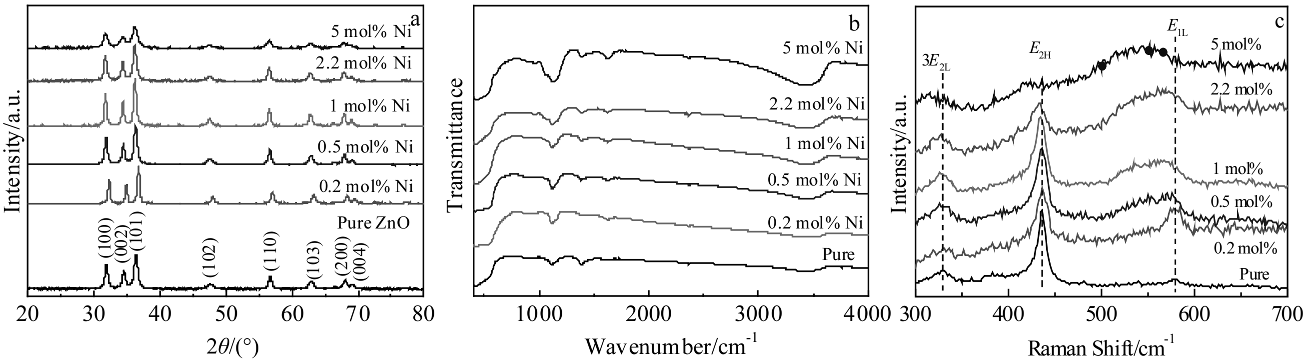

Fig.2 XRD patterns (a), FT-IR infrared spectra (b), and Raman spectra (c) of Ni-doped ZnO at different doping concentrations

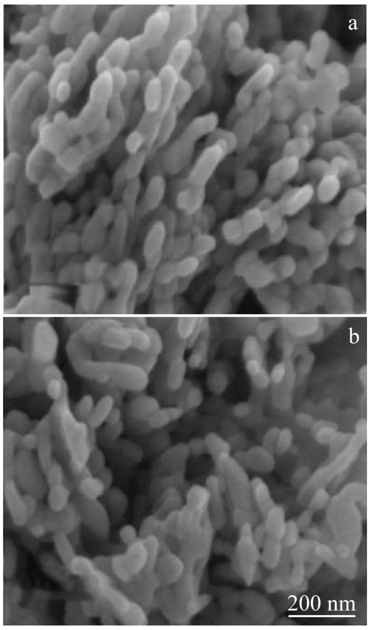

Fig.3 SEM images of pure ZnO (a) and 1 mol% Ni-doped ZnO (b)

eV and 1044.31 eV in Fig.3b[29], respectively. The binding energy position of the spectra closely matches the standard data of zinc oxide. According to Fig.3c, the Ni 2p peak can be resolved into two Gauss peaks similarly: the Ni $2p_{3/2}$ appears at 856.04 eV and the other Ni $2p_{1/2}$ appears at 872.25 eV, indicating that Ni is present in a chemical state of 3+ [28].

2.2 Gas sensing property of Ni-doped ZnO

The gas sensing properties of pure and Ni-doped ZnO were investigated at different operating temperatures so as to find the optimum operating condition for acetone detection. The optimum operating temperature of the pure ZnO and Ni-doped ZnO to 20 μg/g acetone was studied from 200 °C to 440 °C. The results are shown in Fig.5a. Pure and Ni-doped ZnO with different doping concentrations have different optimum operating temperatures. The optimum operating temperature of pure and 0.2 mol% Ni-doped ZnO is 300 °C, while that of others is 340 °C. 1 mol% Ni-doped ZnO shows the highest response to acetone at 340 °C. Therefore the optimum Ni dosage is 1 mol%. Fig.5b represents the selectivity of the 1 mol% Ni doped ZnO, indicating a great selectivity to acetone.

The mechanism of gas sensing of ZnO can be explained by a surface defect model. There is a large amount of oxygen vacancies on the surface of the metal oxide. When a layer of negative oxygen ions is adsorbed on the surface of metal oxide, an electron depletion layer is formed on the surface of the material. It mainly refers to the resistivity of sensitive

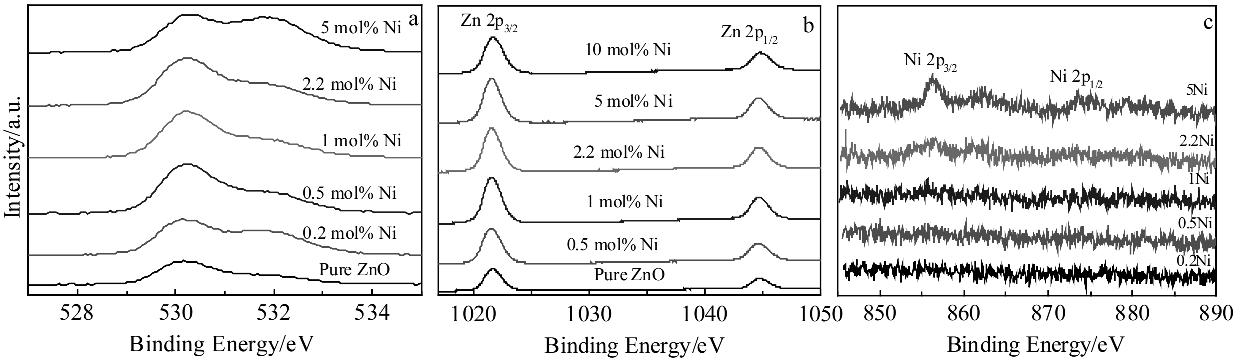

Fig.4 XPS spectra of Ni-doped ZnO: (a) O 1s level, (b) Zn 2p level, and (c) Ni 2p level

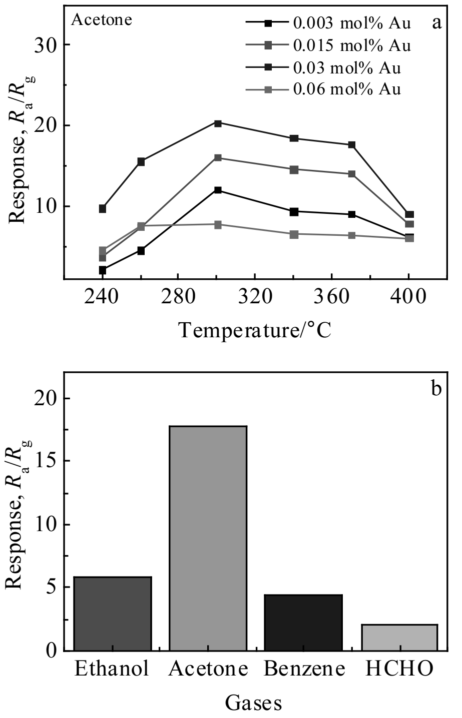

Fig.5 Responses vs operating temperature (a) and selectivity of pure ZnO and Ni-dope ZnO (b) for 20 μg/g acetone

material, which is controlled by the carrier concentration in the depletion layer. In addition to the change of the surface state, the electron transport between the adjacent grains can form a barrier, which is defined as double Schottky barrier. Therefore, the conductivity of the material is determined by the electrical properties of the grain and the transmission of the grain boundaries.

When the ambient is shifted from air to acetone, acetone reacts with the oxygen ions on the surface of the gas sensor. The reaction is shown in Eq.(1)[30]:

$$CH_3COCH_3\ _{(ads)}+8O^-_{(ads)}\rightarrow 3CO_{2(g)}+3H_2O+8e^- \quad (1)$$

Free electrons are released from electron depletion layer at this time contributing to the electrical conductivity increase of the material, and the detection of gas is realized. The ratio of the R_a/R_g is defined as the response, which is an important parameter to measure the sensitivity.

The addition of a proper amount of Ni element in ZnO can improve the sensitivity and selectivity of the gas sensor. From the XRD and Raman characterization, it can be proved that Ni has been successfully incorporated into the ZnO lattice. Based on that, the result of XPS indicates that Ni is present in a chemical state of 3+. More oxygen vacancies appear because Zn^{2+} is substituted by Ni^{3+} according to previous studies[31-34]. The process promotes the adsorption of oxygen and more free electrons are released from electron depletion layer when acetone reacts with the oxygen ions[28,29]. Therefore, the gas sensing properties of ZnO are improved by doping proper concentration of Ni. But excessive doping can cause lattice structure failure, which reduces the gas sensing properties of ZnO[30,31].

2.3 Combination of Ni-doping and Au activation of ZnO sensor

Au was added into 1 mol% Ni-doped ZnO sensor in this study to investigate the combination effect of the two doping methods on acetone gas sensing property of ZnO. Fig.6a shows the 0.03 mol% Au activated material has the highest gas response to 20 μg/g acetone at 300 °C. Fig.6b compares the response of these sensors at optimum operating temperature. We find that Au can enhance the response for acetone.

The response and recovery behaviors are two important characteristics for evaluating the performance of sensors. The response time can be defined as the time needed to reach 90% of its saturated pulse height, while the recovery time is the time needed for the pulse to reach 10% from its base line. Fig.7a depicts the response-recovery characteristics of 0.03 mol% Au activated 1 mol% Ni-doped ZnO sensor to acetone with concentrations varying from 5 μg/g to 100 μg/g at 300 °C. It is represented that the response increases rapidly all the time in the range of 5~100 μg/g (response-recovery time is about 6~8 s) inferring the fast diffusion and reaction of acetone on the sensing film. Fig.7b shows the response of the sensor to 20

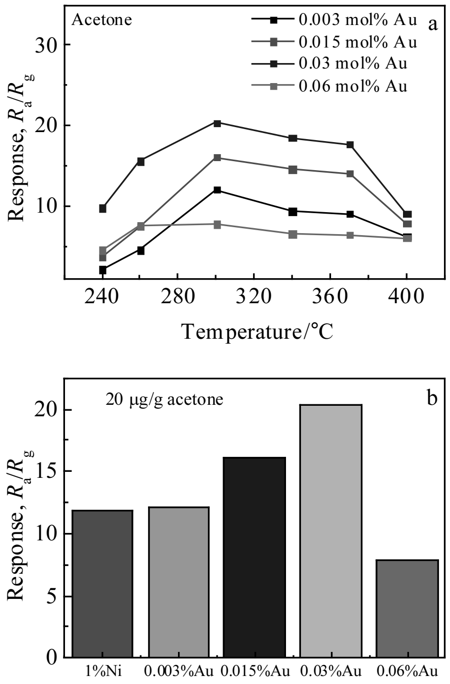

Fig.6 Responses vs operating temperature of Au activated 1 mol% Ni-doped ZnO (a) and the responses of 1 mol% Ni-doped ZnO and Au activated 1 mol% Ni-doped ZnO (b) at optimum operating temperature for 20 μg/g acetone

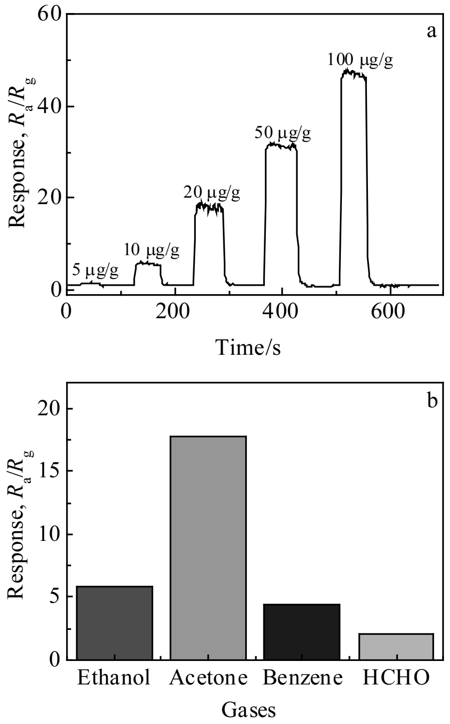

Fig.7 Response-recovery characteristics of 0.03 mol% Au activated 1 mol% Ni-doped ZnO sensor to different acetone concentrations at 300 °C (a) and the response of 0.03 mol% Au activated 1 mol% Ni-doped ZnO sensor to 20 µg/g different gases at 300 °C (b)

µg/g different chemicals at 300 °C and demonstrates that response of acetone excels that of ethanol, formaldehyde and benzene. Among them, the equal concentration response of acetone is almost 3 times higher than those of benzene and ethanol, and 5 times higher than that of formaldehyde, showing the good selectivity to acetone.

The structure of 0.03 mol% Au activated 1 mol% Ni-doped ZnO was explored by SEM, XRD and XPS. The SEM image of the sample is shown in Fig.8a. It can be observed that the morphology of the sample is uniform granulate and the nanoparticles size of about 50 nm. Fig.8b is the XRD pattern of 0.03 mol% Au activated 1 mol% Ni-doped ZnO. The peaks at 38.2° and 44.4° are Au(111) and (200) crystal planes besides the ZnO peaks. The weaker Au peaks are expected because of the relatively small coverage of the nanoparticles[35]. The SEM image and the XRD pattern suggest that 0.03 mol% Au activated 1 mol% Ni-doped ZnO has been successfully synthesized.

The elements and their oxidation states of 0.03 mol% Au activated 1 mol% Ni-dope ZnO were investigated by XPS spectra. Fig.9a shows the Au 4f peaks at 88.5 and 91.0 eV[36], which again illustrate the effective Au decoration on the Ni-doped ZnO nanoparticles. Fig.9b is Zn 2p spectra of Ni-doped ZnO with and without Au decoration. The relative

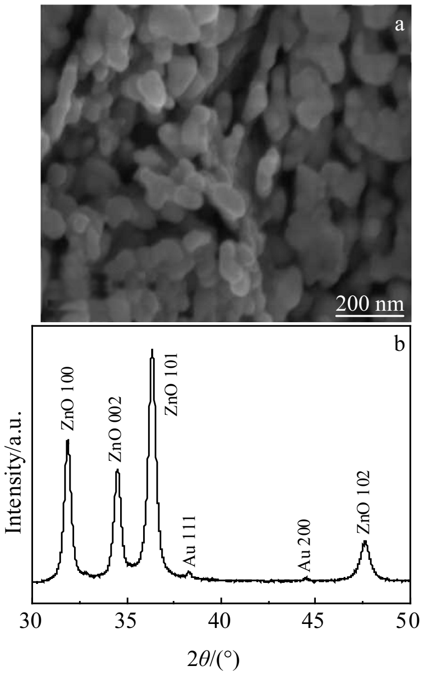

Fig. 8 SEM image (a) and XRD pattern (b) of 0.03 mol% Au activated 1 mol% Ni-doped ZnO sensor

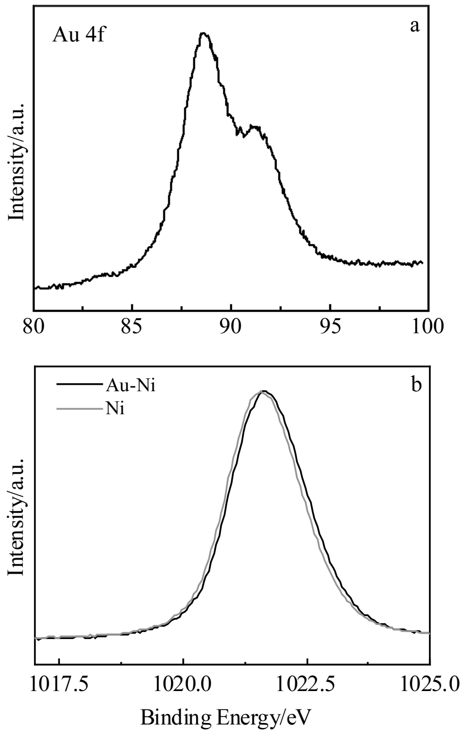

Fig.9 XPS spectra of 0.03 mol% Au activated 1 mol% Ni-doped ZnO sensor: (a) Au4f peak of 0.03 mol% Au activated 1 mol% Ni-doped ZnO sensor, (b) Zn 2p peak of 0.03 mol% Au activated 1 mol% Ni-doped ZnO sensor and 1 mol%

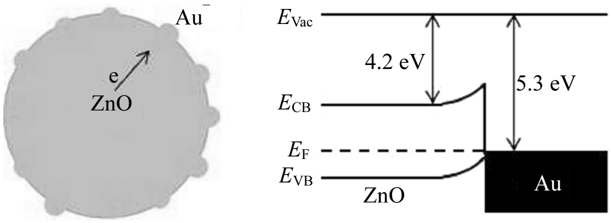

Fig. 10 Mechanism graph of Au activation

shift of Zn 2p peak to higher binding energy is attributed to the effective Au/ZnO heterojunction where electrons will transfer from Ni-doped ZnO to Au due to the relatively higher work function of Au (5.3 eV) than that of ZnO (4.6 eV). This effective heterojunction contributes to the gas response enhancement in Fig.7. This mechanism of Au activation is different from previous Ni doping effect. Au is not incorporated into the ZnO lattice but as the second phase forming the heterojunction on the surface of ZnO nanoparticle (Fig.10). The heterojunction can hold more oxygen ions which further enhance the gas sensing performance.

3 Conclusions

1) The pure and Ni-doped ZnO are prepared by coprecipitation method.

2) Ni dopant (1 mol%) can effectively increase the acetone response of ZnO sensor more than 2- fold.

3) Au can effectively activate 1 mol% Ni-doped ZnO acetone gas sensing material, and 0.03 mol% Au activated 1 mol% Ni-doped ZnO shows the highest response of 17 µg/g to 20 µg/g acetone, and high selectivity over toluene, formaldehyde and ethanol.

References

1 Jeong H M, Kim H J, Ra P *et al. Sensors and Actuators B: Chemical*[J], 2014, 482(5): 489

2 Umar A, Lee J H, Kumar R *et al. Materials & Design*[J], 2016, 105: 16

3 Mote V D, Purushotham Y, Dole B N *et al. Materials & Design*[J], 2016, 96: 99

4 Ismail A A, Harraz F A, Faisal M *et al. Materials & Design*[J], 2016, 530: 538

5 Jin W X, Ma S Y, Tie Z Z *et al. Sensors and Actuators B, B: Chemical*[J], 2015, 213: 171

6 Rebholz J, Dee C, Weimar U *et al. Procedia Engineering*[J], 2015, 120: 83

7 Yang C, Xiao F, Wang J *et al. Sensors and Actuators B: Chemical*[J], 2015, 207: 177

8 Wan X, Wang J, Zhu L *et al. Journal of Materials Chemistry A*[J], 2014, 33(2): 13 641

9 Koh Y K, Bae M H, Cahill D G *et al. Nano Lett*[J], 2010(10): 4363

10 Mavrin B N, Demyanets L N, Zakalukin R M *et al. Physics Letters A*[J], 2010, 374(39): 4054

11 Otaño W，Pantojas V M，Figueroa J M. *MRS Proceedings*[J], 2016, 975: 44

12 Gao J, Liu Q, Gu F *et al. RSC Adv*[J], 2015, 5(29): 22 759

13 Tamvakos A, Calestani D, Tamvakos D *et al. Microchim Acta* [J], 2015, 182(11-12): 1991

14 Losego M D, Grady M E, Sottos N R *et al. Nat Mater*[J], 2012(11): 502

15 Chen T Y, Chen H I, Hsu C S *et al. Sensors and Actuators B: Chemical*[J], 2015, 221: 491

16 Yao M, Hu P, Cao Y *et al. Sensors and Actuators B: Chemical*[J], 2013, 177(2) : 562

17 Xu L, Xing R, Song J *et al. Song Journal of Materials Chemistry C*[J], 2013, 21: 2174

18 Chen Z, Liu L, Lv Y *et al. Energy Microbes Infect*[J], 2016, 5(7): 69

19 Kafle B P, Acharya S, Thapa S *et al. Ceramics International*[J], 2016, 42(1): 1133

20 Ahmed F, Arshi N, Anwar M S *et al. Current Applied Physics*[J], 2013, 13(6): S64

21 Yin M, Liu S. *Materials Chemistry and Physics*[J], 2015, 149-150(150): 344

22 Uddin A S M I, Yaqoob U, Chung G S. *Sensors and Actuators B: Chemical*[J], 2016, 222: 536

23 Li X, Zhou X, Guo H *et al. ACS Appl Mater Interfaces*[J], 2016, 21(6): 18 661

24 Chen W G, Gao T Y, Gan H L *et al. Materials Technology*[J], 2015, 30(6): 356

25 Rambu A P, Ursu L, Iftimie N *et al. Applied Surface Science*[J], 2013, 280(8): 598

26 Mani G K, Rayappan J B B. *Applied Surface Science*[J], 2014, 311(9): 405

27 Zhou H, Li Z. *Materials Chemistry and Physic*[J], 2005, 326: 331

28 Raja K, Ramesh P S, Geetha D *et al. Molecular and Biomolecular Spectroscopy*[J], 2014, 120(4): 19

29 Xu X L, Chen Y, Ma S Y *et al. Sensors and Actuators B: Chemical*[J], 2015, 213: 222

30 Sahay P P. *Journal of Materials Science*[J], 2005, 4383: 4385

31 Bal A K, Singh A, Bedi R K *et al. Sensors and Actuators B: Chemical*[J], 2011, 157(2): 466

32 Sarala Devi G, Bala Subrahmanyam V, Gadkari S C *et al. Journal of Materials Science*[J], 568(1-2): 41

33 Han N, Chai L Y, Wang Q *et al. Journal of Materials Science*[J], 2010, 147(2): 525

34 Yu A, Qian J, Pan H *et al. Journal of Materials Science* [J], 2012, 258(8): 3490

35 Chung F C, Zhu Z, Luo P Y. *Sensors and Actuators B: Chemical*[J], 2014, 199(6): 314

36 Senthilraja A, Krishnakumar B, Subash B *et al. Journal of Industrial and Engineering Chemistry*[J], 2016, 51: 58

共沉淀法制备金、镍掺杂氧化锌的丙酮气敏性能探究

王劲枭[1,2]，杨　军[1]，韩　宁[2, 3]，杨建锋[4]
(1. 西安建筑科技大学，陕西 西安 710055)
(2. 中国科学院过程工程研究所 多相复杂系统国家重点实验室，北京 100190)
(3. 中国科学院厦门城市环境研究所 区域大气环境研究卓越创新中心，福建 厦门 361021)
(4. 西安交通大学 金属材料强度国家重点实验室，陕西 西安 710049)

摘　要：利用共沉淀法制备了纯氧化锌和镍掺杂氧化锌。比较了不同 Ni 掺杂浓度对 ZnO 丙酮气敏传感器性能的影响。结果表明，1 mol% Ni 掺杂 ZnO 具有最高的丙酮传感性能，其对 20 μg/g 丙酮的响应值达到 12。在此基础上，添加金作为异质结进一步激活氧化锌传感材料。实验结果表明，0.03 mol% Au 活化 1 mol% Ni 掺杂的 ZnO 表现出最高的丙酮气敏响应，对 20 μg/g 丙酮的响应值达到 17。同时，该气敏材料保持了对乙醇、甲醛及苯的高选择性，以及对丙酮的快速响应恢复时间(<10 s)。

关键词：丙酮气敏传感器；镍掺杂氧化锌；金活化；响应恢复时间

作者简介：王劲枭，男，1992 年生，硕士生，西安建筑科技大学冶金工程学院，陕西 西安 710055，E-mail: 1371366004@qq.com